Joint product numerical range and geometry of reduced density matrices

Jianxin Chen,[1] Cheng Guo,[2] Zhengfeng Ji,[3,4] Yiu-Tung Poon,[5] Nengkun Yu,[6,3,7] Bei Zeng,[6,7] and Jie Zhou[8]

[1] *Joint Center for Quantum Information and Computer Science, University of Maryland, College Park, Maryland, USA*
[2] *Institute for Advanced Study, Tsinghua University, Beijing, China*
[3] *Centre for Quantum Computation & Intelligent Systems, School of Software, Faculty of Engineering and Information Technology, University of Technology Sydney, Sydney, Australia*
[4] *State Key Laboratory of Computer Science, Institute of Software, Chinese Academy of Sciences, Beijing, China*
[5] *Department of Mathematics, Iowa State University, Ames, Iowa, USA.*
[6] *Institute for Quantum Computing, University of Waterloo, Waterloo, Ontario, Canada*
[7] *Department of Mathematics & Statistics, University of Guelph, Guelph, Ontario, Canada*
[8] *Perimeter Institute for Theoretical Physics, Waterloo, Ontario, Canada*

arXiv:1606.07422v1 [quant-ph] 23 Jun 2016

The reduced density matrices of a many-body quantum system form a convex set, whose three-dimensional projection Θ is convex in $\mathbb{R}^3$. The boundary $\partial\Theta$ of Θ may exhibit nontrivial geometry, in particular ruled surfaces. Two physical mechanisms are known for the origins of ruled surfaces: symmetry breaking and gapless. In this work, we study the emergence of ruled surfaces for systems with local Hamiltonians in infinite spatial dimension, where the reduced density matrices are known to be separable as a consequence of the quantum de Finetti's theorem. This allows us to identify the reduced density matrix geometry with joint product numerical range Π of the Hamiltonian interaction terms. We focus on the case where the interaction terms have certain structures, such that ruled surface emerge naturally when taking a convex hull of Π. We show that, a ruled surface on $\partial\Theta$ sitting in Π has a gapless origin, otherwise it has a symmetry breaking origin. As an example, we demonstrate that a famous ruled surface, known as the oloid, is a possible shape of Θ, with two boundary pieces of symmetry breaking origin separated by two gapless lines.

I. INTRODUCTION

In a natural many-body quantum system, the Hamiltonian H usually involves only two-body interactions. Consequently, for any many-body wave function $|\psi\rangle$, its energy $E_\psi = \langle\psi|H|\psi\rangle$ only depends on the two-particle reduced density matrix (2-RDM) of $|\psi\rangle$. In case H depends on some parameters $\vec{\lambda}$, the ground state energy $E_0(\vec{\lambda})$ of the system may exhibit non-analylic behaviour while $\vec{\lambda}$ change smoothly, where a quantum phase transition occurs. Since the energy E_ψ only depends on its 2-RDMs, it is much desired that the geometry of the 2-RDMs may capture such a sudden change in ground state energy $E_0(\vec{\lambda})$.

The set of all 2-RDMs is known to be convex, however its shape is notoriously difficult to characterize in general. Since 1960s, how to characterize this convex set has been a central topic of research in the field of quantum marginal problem and N-representability problem [1–5]. The recent development in quantum information theory has shown that the characterization of the 2-RDMs is a hard problem even with the existence of a quantum computer [6–8]. Nevertheless, many practical approaches are developed to characterize the properties of 2-RDMs, and to retrieve useful information that reflects the physical properties of the system [9, 10].

One important idea is to study the properties of 2-RDMs is by looking at the two- and three- dimensional projections [4, 5, 9, 10]. Since these projections are convex sets in $\mathbb{R}^2$ and $\mathbb{R}^3$ respectively, the hope is that the properties of the different quantum phases can be visually available. Interestingly, it has been shown that a flat portion of the two-dimensional projection can already signal first-order phase transitions [11, 12]. However, for continuous phase transitions, two-dimensional projections contain no information, and one needs to look further at the three-dimensional projections.

In [12] it is observed that the emergence of ruled surfaces on the boundary of the three-dimensional projections of 2-RDMs can be a signal of symmetry breaking phase. With a generalization to non-thermodynamic observables, the ruled surfaces can also signal the symmetry protected topological phase [13]. Very recently, it is also observed that gapless systems can also lead to ruled surfaces, and two examples of such systems are discussed, which are both interacting many-body bosonic systems [14].

It was Gibbs in 1870's who first proposed the deep connection between ruled surfaces on the boundary of certain convex body and phase transitions [15–18], in the context of classical thermodynamics, which reflects a fundamental property of thermodynamic stability. Although the convex set considered here is in terms of quantum many-body physics, and the connection is between ruled surface on the projection of RDMs and quantum phase transitions, it nevertheless indicates that the convex geometry approach is a fundamental and universal idea.

In both classical and quantum cases, one fundamental question is in the reverse direction: that is, what kind of ruled surfaces are actually possible? In other words,

what shapes of ruled surfaces may actually correspond to a practical quantum system? This question is, of course, too hard in general, but opens some interesting possibilities. For instance, one may ask whether the oloid, being a famous ruled surface in $\mathbb{R}^3$, can be a three-dimensional projection of some convex set of 2-RDMs.

This oloid idea may sound unrealistic at the first sight. Surprisingly, we will show that this is in fact possible. We will develop a method that systematically leads to many other possibilities of ruled surface for the three-dimensional projections of 2-RDMs. We start from a fact that although the geometry of 2-RDMs are in general hard to characterize, there is one situation it is provably easy: that is, for an infinite spatial dimensional system, the 2-RDMs are known to be separable, due to the celebrated quantum de Finetti's theorem [19–21].

This simplification to only separable states then allows us to study the geometry of 2-RDMs with a mathematical concept, called joint product numerical range [22–27], denoted by Π, of the Hamiltonian interaction terms. Π includes all the extreme points of the three-dimensional projections of 2-RDMs, and the projection itself, denoted by Θ, is a convex hull of Π. We then focus on the cases where the interaction terms have certain structures, such that ruled surfaces emerge naturally when taking a convex hull of Π. We show that, for a ruled surface on the boundary of Θ, denoted by $\partial\Theta$, if it also sits in Π, then it has a gapless origin, otherwise it has a symmetry breaking origin.

II. REDUCED DENSITY MATRIX GEOMETRY AND ITS PROJECTIONS

We consider many-body systems with N-particles, and single-particle dimension d (i.e. single-particle Hilbert space $\mathbb{C}^d$). For a many-body Hamiltonian $H(\vec{\lambda})$, we discuss the case where $\vec{\lambda} = (\lambda_1, \lambda_2, \lambda_3)$, and

$$H(\vec{\lambda}) = \sum_{i=1}^{3} \lambda_i H_i. \tag{1}$$

Here each $H_i = \sum_j h_{j,i}$, and $h_{j,i}$ involves at most two-body interactions. Therefore, for any many-body wave function of the system, only its 2-RDM is of relevance to our discussion. In other words, we are interested in the set of all possible 2-RDMs of the many-body wave functions.

In practice, the structure of the 2-RDMs only depends on the interaction pattern of H [28]. That is, usually, the interaction terms in H_i involves only 'nearest-neighbour' interactions depending on the spatial geometry of the system. In this work we consider a special case, where the spatial geometry is infinite-dimensional. That is, each single particle in the system has infinitely-many neighbours. Consequently, we are in the limit of infinite number of particles, i.e. $N \to \infty$.

For simplicity we consider a particular case that the system has $\mathcal{A}$, $\mathcal{B}$ sub-lattices and with translational symmetry, and the H_is only involve nearest-neighbour interactions. That is, for $H_i = \sum_j h_{j,i}$, each $h_{j,i}$ involves at most two-body interactions and acts the same for each nearest neighbour AB particles. And for any particle A in the sublattice $\mathcal{A}$ and particle B in the sublattice $\mathcal{B}$ that are neighbours, the corresponding reduced density matrix ρ_{AB} (of any state of the N-particle system) are the same. In other words, ρ_{AB} contains all the information of interest of 2-RDMs of the physical system.

In the $N \to \infty$ limit, the quantum de Finetti's theorem guarantees that ρ_{AB} is separable [19, 20]. In other words, ρ_{AB} can always be written as

$$\rho_{AB} = \sum_j c_j |\psi^j_{AB}\rangle\langle\psi^j_{AB}|\,, \tag{2}$$

with $c_j \geq 0$, $\sum_j c_j = 1$, and each $|\psi^j_{AB}\rangle \in \mathbb{C}^d \otimes \mathbb{C}^d$ is a product state of the form

$$|\psi^j_{AB}\rangle = |\alpha^j\rangle \otimes |\beta^j\rangle\,, \tag{3}$$

with $|\alpha^j\rangle, |\beta^j\rangle \in \mathbb{C}^d$.

Therefore, to study the three-dimensional projection of the 2-RMDs, we are in fact considering the three-dimensional projection of the set of all the two-particle separable state ρ_{AB}s. This projection is given by the set of points $(x, y, z) \in \mathbb{R}^3$, where

$$x = \mathrm{Tr}(H_1\rho_{AB}),\ y = \mathrm{Tr}(H_2\rho_{AB}),\ z = \mathrm{Tr}(H_3\rho_{AB}), \tag{4}$$

And the projection of the extreme points of the set of all separable state ρ_{AB}s, which are product states $|\alpha\rangle \otimes |\beta\rangle$, is given by the set of points $(x, y, z) \in \mathbb{R}^3$, where

$$\begin{aligned} x &= (\langle\alpha| \otimes \langle\beta|)H_1(|\alpha\rangle \otimes |\beta\rangle), \\ y &= (\langle\alpha| \otimes \langle\beta|)H_2(|\alpha\rangle \otimes |\beta\rangle), \\ z &= (\langle\alpha| \otimes \langle\beta|)H_3(|\alpha\rangle \otimes |\beta\rangle). \end{aligned} \tag{5}$$

And in fact we only need to consider the terms $h_{j,i}$ of H_i that act non-trivially on particles AB. In other words, we can equivalently consider H_i as Hermitian operators acting on $\mathbb{C}^d \otimes \mathbb{C}^d$, without confusion we use H_i to mean its 'energy per particle' version acting on two particles AB (hence H_i is bounded) [14]. This then allows us to connect our discussions to some mathematical concepts, namely certain kind of joint numerical ranges of H_is. For simplicity we only consider $d = 2$ (i.e. qubit) case in this work. However, the method we discuss is general and can extend to the $d > 2$ cases.

III. PRODUCT NUMERICAL RANGE

We consider a two-qubit system AB, with Hilbert space $\mathbb{C}^2 \otimes \mathbb{C}^2$. Let S be the set of normalized $|\psi\rangle \in$

$\mathbb{C}^2 \otimes \mathbb{C}^2$ (i.e. $\langle\psi|\psi\rangle = 1$). For any three 4×4 Hermitian operators H_1, H_2, H_3, the joint numerical range [29] of H_1, H_2, H_3 is given by

$$\begin{aligned}&\Lambda(H_1, H_2, H_3) = \\ &\{(\langle\psi|H_1|\psi\rangle, \langle\psi|H_2|\psi\rangle, \langle\psi|H_3|\psi\rangle)||\psi\rangle \in S\}. \end{aligned} \quad (6)$$

One important property of $\Lambda(H_1, H_2, H_3)$ is given in [29] that is summarized below.

Fact 1 *$\Lambda(H_1, H_2, H_3) \subset \mathbb{R}^3$ is convex.*

Let S_Π be the set of product states $|\phi\rangle = |\alpha\rangle \otimes |\beta\rangle \in S$ with $|\alpha\rangle, |\beta\rangle \in \mathbb{C}^2$, the product numerical range of H_1, H_2, H_3 is given by

$$\begin{aligned}&\Pi(H_1, H_2, H_3) = \\ &\{(\langle\phi|H_1|\phi\rangle, \langle\phi|H_2|\phi\rangle, \langle\phi|H_3|\phi\rangle)||\phi\rangle \in S_\Pi\}. \end{aligned} \quad (7)$$

It is known that $\Pi(H_1, H_2, H_3)$ is in general not convex [30].

Consider any separable state $\rho_{AB} = \sum_j c_j |\psi_{AB}^j\rangle\langle\psi_{AB}^j|$ with each $|\psi_{AB}^j\rangle = |\alpha^j\rangle \otimes |\beta^j\rangle$ a product state. The separable numerical range of H_1, H_2, H_3 is given by

$$\begin{aligned}&\Theta(H_1, H_2, H_3) = \\ &\{(\mathrm{Tr}\, H_1\rho_{AB}, \mathrm{Tr}\, H_2\rho_{AB}, \mathrm{Tr}\, H_3\rho_{AB}) \\ &|\rho_{AB} \text{ separable}\}. \end{aligned} \quad (8)$$

It is clear that $\Theta(H_1, H_2, H_3)$ is the convex hull of $\Pi(H_1, H_2, H_3)$, hence is convex, with all the extreme points in $\Pi(H_1, H_2, H_3)$. In general

$$\Theta(H_1, H_2, H_3) \subseteq \Lambda(H_1, H_2, H_3), \quad (9)$$

and in most cases, $\Theta(H_1, H_2, H_3)$ does not equal to $\Lambda(H_1, H_2, H_3)$.

A. The physical origin of boundary ruled surfaces

For any product state $|\psi\rangle = |\alpha\rangle \otimes |\beta\rangle$ and the Hamiltonian $H(\vec{\lambda}) = \sum_{i=1}^3 \lambda_i H_i$, its energy is

$$E_\psi(\vec{\lambda}) = x\lambda_1 + y\lambda_2 + z\lambda_3 \geq E_0(\vec{\lambda}), \quad (10)$$

where x, y, z are given in Eq. (5) and $E_0(\vec{\lambda})$ is the ground state energy of $H(\vec{\lambda})$. Since $\Theta(H_1, H_2, H_3)$ is convex, for each $\vec{\lambda}$, the Hamiltonian $H(\vec{\lambda})$ can be interpreted as a supporting plane of $\Theta(H_1, H_2, H_3)$ with normal vector given by $\vec{\lambda} = (\lambda_1, \lambda_2, \lambda_3)$ [11, 31].

Our main focus is on the boundary of $\Theta(H_1, H_2, H_3)$, which is denoted by $\partial\Theta(H_1, H_2, H_3)$. Generically, an exposed point P_e on $\partial\Theta(H_1, H_2, H_3)$ has a unique product state pre-image in $\Pi(H_1, H_2, H_3)$. Physically, this means that the corresponding Hamiltonian $H(\vec{\lambda}) = \sum_{i=1}^3 \lambda_i H_i$ (i.e. the supporting plane of $\Theta(H_1, H_2, H_3)$ that intersects $\partial\Theta(H_1, H_2, H_3)$ at the point P_e) has a unique product ground state.

The boundary of $\partial\Theta(H_1, H_2, H_3)$ can also be flat. And in most cases this plat portion is completely flat, i.e. it is a part of a plane, which is an area of the intersection of the corresponding supporting plane of $\Theta(H_1, H_2, H_3)$ with $\partial\Theta(H_1, H_2, H_3)$. The boundary of the area has infinitely many product state pre-images in $\Pi(H_1, H_2, H_3)$. Physically, this means that the corresponding Hamiltonian is gapless.

A nontrivial case is that the flat portion on $\partial\Theta(H_1, H_2, H_3)$ is not a part of a plane, but rather a ruled surface. That is, for any point P_e on $\partial\Theta(H_1, H_2, H_3)$, there is a line segment L passing P_e that is also on the surface. Physically, there are two known origins of ruled surfaces: 1) symmetry breaking [12] and 2) Gapless [14].

In general, one cannot tell the physical origins of the ruled surfaces solely from the shape of $\partial\Theta(H_1, H_2, H_3)$ [14]. One idea to tell the difference is to look at the finite scaling of RDM geometry [14]. Here we would like to connect these physical origins to the properties of joint product numerical range $\Pi(H_1, H_2, H_3)$.

Consider any line segment L on $\partial\Theta(H_1, H_2, H_3)$, with two end points P_a and P_b. In case there is no plane area on $\partial\Theta(H_1, H_2, H_3)$ that contains L, then there is a supporting plane of $\Theta(H_1, H_2, H_3)$ that intersects $\partial\Theta(H_1, H_2, H_3)$ only at L, with normal vector $\vec{\lambda} = (\lambda_1, \lambda_2, \lambda_3)$.

It is clear that $P_a, P_b \in \Pi(H_1, H_2, H_3)$. Here are two possible cases: 1) L is not in $\Pi(H_1, H_2, H_3)$, 2) $L \subset \Pi(H_1, H_2, H_3)$. For case 1), generically, each P_a (or P_b) has a unique product state pre-image in $\Pi(H_1, H_2, H_3)$. Consequently, the corresponding Hamiltonian $H = \sum_{i=1}^3 \lambda_i H_i$ has degenerate product ground states. For case 2), each point on L has a product state pre-image in $\Pi(H_1, H_2, H_3)$, so L has infinitely many product state pre-images in $\Pi(H_1, H_2, H_3)$. Consequently, the corresponding Hamiltonian $H = \sum_{i=1}^3 \lambda_i H_i$ is gapless.

If there is a piece of ruled surface on $\partial\Theta(H_1, H_2, H_3)$ which is not in $\Pi(H_1, H_2, H_3)$ (except the boundary of the piece), then the corresponding Hamiltonian $H = \sum_{i=1}^3 \lambda_i H_i$ maintains its round state degeneracy when $\vec{\lambda}$ varies. In other words, for a range of parameters $\vec{\lambda}$, $H = \sum_{i=1}^3 \lambda_i H_i$ has stable ground state degeneracy (along the parameter-changing direction), with product ground states. This is a typical feature of symmetry breaking. In this sense, a ruled surface on $\partial\Theta(H_1, H_2, H_3)$ that is not in $\Pi(H_1, H_2, H_3)$ has a symmetry breaking origin. In comparison, if the ruled surface piece is in $\Pi(H_1, H_2, H_3)$, then it has a gapless origin.

We summarize our observation as the following.

Observation 1 *A ruled surface on*

$$\Pi(H_1, H_2, H_3) \cap \partial\Theta(H_1, H_2, H_3) \tag{11}$$

has a gapless origin. Otherwise, a ruled surface on $\partial\Theta(H_1, H_2, H_3)$ *that is not in* $\Pi(H_1, H_2, H_3)$ *has a symmetry breaking origin.*

This observation gives us a general method to study the physics of the reduced density matrix geometry $\Theta(H_1, H_2, H_3)$. That is, for any given system $H = \sum_{i=1}^{3} \lambda_i H_i$, by comparing $\Theta(H_1, H_2, H_3)$ with $\Pi(H_1, H_2, H_3)$, one should be able to get quantum phases and phase transition informations by solely looking at the geometry of $\Theta(H_1, H_2, H_3)$ and $\Pi(H_1, H_2, H_3)$.

B. The block diagonal Hamiltonians

Compared to exposed points and completely flat areas, ruled surfaces are much less possible to find in generic systems. It usually requires certain structure of $H = \sum_{i=1}^{3} \lambda_i H_i$, e.g. symmetry. In order to understand the possible ruled surface shapes on $\partial\Theta(H_1, H_2, H_3)$ and their physical possible origins, we would like to look at Hamiltonians with structure. Geometrically, flat portions on $\partial\Theta(H_1, H_2, H_3)$ may be obtained from the convex hull of two (not flat) objects. This inspires us to consider the case where H_1, H_2, H_3 are block diagonal, i.e.

$$H_i = \begin{pmatrix} H_i^a & O \\ O & H_i^b \end{pmatrix}, \ i = 1, 2, 3\,, \tag{12}$$

where H_i^a, H_i^b are 2×2, and O is the 2×2 zero matrix.

Denote the joint numerical range of H_1^a, H_2^a, H_3^a by $\Lambda(H_1^a, H_2^a, H_3^a)$ and the joint numerical range of H_1^b, H_2^b, H_3^b by $\Lambda(H_1^b, H_2^b, H_3^b)$. One important property of joint numerical range of block diagonal matrices is the following.

Fact 2 $\Lambda(H_1, H_2, H_3)$ *is the convex hull of* $\Lambda(H_1^a, H_2^a, H_3^a)$ *and* $\Lambda(H_1^b, H_2^b, H_3^b)$ *[32].*

What we need is the shape of $\Theta(H_1, H_2, H_3)$, not $\Lambda(H_1, H_2, H_3)$. They are in general two very different sets, i.e. the equality in Eq. (9) in general does not hold. In the special case of block diagonal matrices, however, we can show that these two sets coincide.

Observation 2 *For block diagonal* H_1, H_2, H_3,

$$\Theta(H_1, H_2, H_3) = \Lambda(H_1, H_2, H_3) \tag{13}$$

To show why it is the case, let $H_i = \begin{pmatrix} H_i^a & O \\ O & H_i^b \end{pmatrix}$, for $i = 1, 2, 3$. Suppose $|\alpha\rangle \in \mathbb{C}^2$. Then

$$\langle\alpha|H_i^a|\alpha\rangle = (\langle 0| \otimes \langle\alpha|) H_i (|0\rangle \otimes |\alpha\rangle)\,. \tag{14}$$

Similarly,

$$\langle\alpha|H_i^b|\alpha\rangle = (\langle 1| \otimes \langle\alpha|) H_i (|1\rangle \otimes |\alpha\rangle)\,. \tag{15}$$

Therefore,

$$\Lambda(H_1^a, H_2^a, H_3^a),\ \Lambda(H_1^b, H_2^b, H_3^b) \subseteq \Pi(H_1, H_2, H_3)\,. \tag{16}$$

Since

$$\begin{aligned} &\Theta(H_1, H_2, H_3) \\ &= \text{conv}\ \Pi(H_1, H_2, H_3) \subseteq \Lambda(H_1, H_2, H_3) \\ &= \text{conv}\ \{\Lambda(H_1^a, H_2^a, H_3^a),\ \Lambda(H_1^b, H_2^b, H_3^b)\}\,, \end{aligned} \tag{17}$$

we have $\Theta(H_1, H_2, H_3) = \Lambda(H_1, H_2, H_3)\,.$

C. The oloid

As an example, let

$$H_1^a = \begin{pmatrix} 0 & 1 \\ 1 & 0 \end{pmatrix},\ H_2^a = \begin{pmatrix} 0 & -i \\ i & 0 \end{pmatrix},\ H_3^a = \begin{pmatrix} 0 & 0 \\ 0 & 0 \end{pmatrix}, \tag{18}$$

then $\Lambda(H_1^a, H_2^a, H_3^a)$ is the disk $\{(x, y, 0) \in \mathbb{R}^3 : x^2 + y^2 \leq 1\}$. Similarly, if

$$H_1^b = \begin{pmatrix} 1 & 1 \\ 1 & 1 \end{pmatrix},\ H_2^b = \begin{pmatrix} 0 & 0 \\ 0 & 0 \end{pmatrix},\ H_3^b = \begin{pmatrix} 0 & -i \\ i & 0 \end{pmatrix}, \tag{19}$$

then $\Lambda(H_1^b, H_2^b, H_3^b)$ is the disk $\{(x, 0, z) \in \mathbb{R}^3 : (x-1)^2 + z^2 \leq 1\}$. A plot of these two disks is given in Fig. 1.

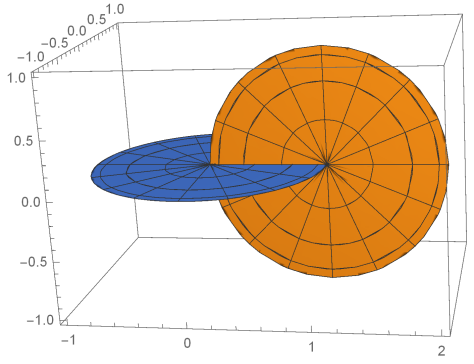

FIG. 1. The two disks corresponding to $\Lambda(H_1^a, H_2^a, H_3^a)$ and $\Lambda(H_1^b, H_2^b, H_3^b)$.

Therefore,

$$\begin{aligned} &\Theta(H_1, H_2, H_3) = \\ &\text{conv}\ \{\Lambda(H_1^a, H_2^a, H_3^a),\ \Lambda(H_1^b, H_2^b, H_3^b)\} \end{aligned} \tag{20}$$

is the so called 'oloid' [33]. A illustration of the oloid is given in Fig. 2.

To obtain the joint product numerical range $\Pi(H_1, H_2, H_3)$, suppose

$$|\alpha\rangle = u_1|0\rangle + u_2|1\rangle \tag{21}$$

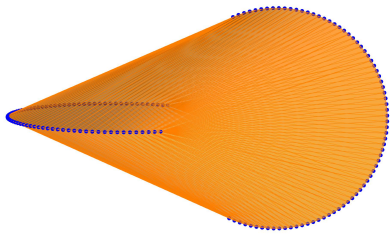

FIG. 2. An Oloid.

with $|u_1|^2 + |u_2|^2 = 1$, and

$$|\beta\rangle = r|0\rangle + \sqrt{1-r^2}e^{it}|1\rangle \tag{22}$$

with $0 \le r \le 1$ and $0 \le t \le 2\pi$. Then

$$\begin{aligned}
&(\langle\alpha| \otimes \langle\beta|)(H_1, H_2, H_3)(|\alpha\rangle \otimes |\beta\rangle) \\
=\ & |u_1|^2(2r\sqrt{1-r^2}\cos t, 2r\sqrt{1-r^2}\sin t, 0) \\
+\ & |u_2|^2(1 + 2r\sqrt{1-r^2}\cos t, 0, 2r\sqrt{1-r^2}\sin t)
\end{aligned} \tag{23}$$

Therefore, let $|u_1|^2 = s_1$, $2r\sqrt{1-r^2} = s_2$, we have

$$\begin{aligned}
&\Pi(H_1, H_2, H_3) = \\
&\{(1 - s_1 + s_2\cos t, s_1 s_2 \sin t, (1-s_1)s_2 \sin t) : \\
&0 \le s_1,\ s_2 \le 1,\ 0 \le t \le 2\pi\}\,.
\end{aligned} \tag{24}$$

We illustrate $\Pi(H_1, H_2, H_3)$ in Fig. 3.

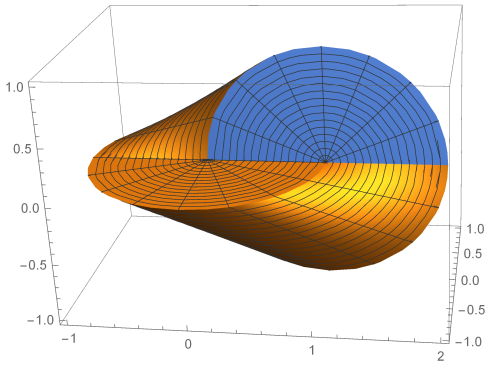

FIG. 3. $\Pi(H_1, H_2, H_3)$ for oloid.

We are interested in the shape of $\Pi(H_1, H_2, H_3) \cap \partial\Theta(H_1, H_2, H_3)$. Since the oloid is a developable surface, we can expand its boundary to put on a plane, as shown in Fig. 4. The intersection of $\Pi(H_1, H_2, H_3)$ with $\partial\Theta(H_1, H_2, H_3)$ contains all the curved parts of the boundary (i.e. boundaries of the two disks). In addition, it also contains two lines shown as the red lines in Fig. 4. These two red lines cut $\partial\Theta(H_1, H_2, H_3)$ into two pieces of ruled surfaces, each of which corresponds to a symmetry breaking phase as discussed in Sec. IIIA. That is, the physical system $H(\vec{\lambda}) = \sum_{i=1}^{3} \lambda_i H_i$ has two symmetry breaking phases separated by two gapless transition points (that correspond to the two red lines in Fig. 4).

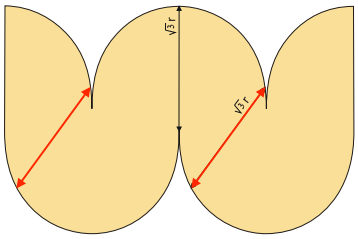

FIG. 4. The developable surface of the oloid. The two red lines are in $\Pi(H_1, H_2, H_3) \cap \partial\Theta(H_1, H_2, H_3)$. Figure modified from https://en.wikipedia.org/wiki/Oloid.

IV. THE SYMMETRIC CASE AND BOSONIC SYSTEMS

We can also consider the product numerical range in the symmetric case. That is, instead of considering product state of the form $|\alpha\rangle \otimes |\beta\rangle$, we restrict ourselves in the case of $|\alpha\rangle \otimes |\alpha\rangle$, and the H_is are supported on the symmetric subspace of $\mathbb{C}^2 \otimes \mathbb{C}^2$. For the symmetric case, we denote the corresponding joint product numerical range by $\Pi_+(H_1, H_2, H_3)$, and the joint separable numerical range by $\Theta_+(H_1, H_2, H_3)$. Physically, we are dealing with a many-body bosonic system with symmetric wavefunctions in the $N \to \infty$ limit, where the reduced density matrices of the wave function of the system is also known to be separable due to the quantum de Finetti's theorem [21].

We consider $\Pi_+(H_1, H_2, H_3)$ that is given by the set of points $(x, y, z) \in \mathbb{R}^3$, where

$$\begin{aligned}
x &= \langle\alpha^{\otimes 2}|H_1|\alpha^{\otimes 2}\rangle = \mathrm{Tr}(H_1|\alpha^{\otimes 2}\rangle\langle\alpha^{\otimes 2}|), \\
y &= \langle\alpha^{\otimes 2}|H_2|\alpha^{\otimes 2}\rangle = \mathrm{Tr}(H_2|\alpha^{\otimes 2}\rangle\langle\alpha^{\otimes 2}|), \\
z &= \langle\alpha^{\otimes 2}|H_3|\alpha^{\otimes 2}\rangle = \mathrm{Tr}(H_3|\alpha^{\otimes 2}\rangle\langle\alpha^{\otimes 2}|)\,.
\end{aligned} \tag{25}$$

Here $|\alpha\rangle \in \mathbb{C}^2$ is any single qubit state.

We can parameterize

$$|\alpha\rangle\langle\alpha| = \frac{1}{2}(I + rX + sY + tZ)\,, \tag{26}$$

and $\vec{r} = (r, s, t)^T$, with $\vec{r}^T\vec{r} = 1$.

And each H_i can be written in the Pauli basis as

$$\begin{aligned} H_i &= c_{0,i} + c_{xx,i} X\otimes X + c_{yy,i} Y\otimes Y + c_{zz,i} Z\otimes Z \\ &+ c_{xy,i}(X\otimes Y + Y\otimes X) + c_{x,i}(X\otimes I + I\otimes X) \\ &+ c_{yz,i}(Y\otimes Z + Z\otimes Y) + c_{y,i}(Y\otimes I + I\otimes Y) \\ &+ c_{xz,i}(X\otimes Z + Z\otimes X) + c_{z,i}(Z\otimes I + I\otimes Z) \end{aligned} \tag{27}$$

With this parameterization, our joint product numerical range of H_1, H_2, H_3 becomes the set of points in $\mathbb{R}^3$ given by

$$(f_1(r,s,t), f_2(r,s,t), f_3(r,s,t))\,, \tag{28}$$

where each f_i is a polynomial of r, s, t of degree at most 2, with the constraint $r^2 + s^2 + t^2 = 1$.

A. The homogenous case

We first consider the simple case where the f_is are homogenous polynomials of r, s, t, i.e. $c_{0,i} = c_{x,i} = c_{y,i} = c_{z,i} = 0$. Hence we can rewrite

$$x = \vec{r}^T M_1 \vec{r},\ y = \vec{r}^T M_2 \vec{r},\ z = \vec{r}^T M_3 \vec{r}, \tag{29}$$

where

$$M_i = \begin{pmatrix} c_{xx,i} & d_{xy,i} & d_{xz,i} \\ d_{xy,i} & c_{yy,i} & d_{yz,i} \\ d_{xz,i} & d_{yz,i} & c_{zz,i} \end{pmatrix} \tag{30}$$

is a real symmetric matrix, for $i = 1, 2, 3$.

Now consider the operator

$$M = uM_1 + vM_2 + wM_3\,, \tag{31}$$

which is a real symmetric matrix, whose eigenvectors can be all real.

Notice that

$$\Pi_+(H_1, H_2, H_3) = \{(\vec{r}^T M_1 \vec{r}, \vec{r}^T M_2 \vec{r}, \vec{r}^T M_3 \vec{r})\}\,, \tag{32}$$

for all $\vec{r}^T \vec{r} = 1$, is the real version of the joint numerical range of (M_1, M_2, M_3). To compare with the joint numerical range of (M_1, M_2, M_3), we denote

$$\Lambda_{\mathbb{R}}(M_1, M_2, M_3) = \{(\vec{r}^T M_1 \vec{r}, \vec{r}^T M_2 \vec{r}, \vec{r}^T M_3 \vec{r})\}. \tag{33}$$

Although $\Lambda_{\mathbb{R}}(M_1, M_2, M_3)$ may not be convex [29], we are going to show that every point in $\Lambda(M_1, M_2, M_3)$ is a convex combination of (at most) two points in $\Lambda_{\mathbb{R}}(M_1, M_2, M_3)$. Therefore, the extreme points of $\Lambda(M_1, M_2, M_3)$ lie in $\Lambda_{\mathbb{R}}(M_1, M_2, M_3)$.

Suppose M is real and symmetric $n \times n$ matrix, and $|v\rangle \in \mathbb{C}^n$ satisfies $\langle v|v\rangle = 1$. Let

$$|v\rangle = |x\rangle + i|y\rangle\,, \tag{34}$$

where $|x\rangle,\ |y\rangle \in \mathbb{R}^n$. Then

$$\langle v|v\rangle = 1 \Rightarrow \langle x|x\rangle + \langle y|y\rangle = 1\,. \tag{35}$$

We have

$$\begin{aligned} \langle v|M|v\rangle &= (\langle x| - i\langle y|)M(|x\rangle + i|y\rangle) \\ &= \langle x|M|x\rangle + \langle y|M|y\rangle\,. \end{aligned} \tag{36}$$

If $|x\rangle$ or $|y\rangle$ is the zero vector, then

$$\langle v|M|v\rangle \in \Lambda_{\mathbb{R}}(M_1, M_2, M_3). \tag{37}$$

Suppose both $|x\rangle$ and $|y\rangle$ are nonzero. Let $t = \sqrt{\langle x|x\rangle}$, and

$$|x'\rangle = \frac{1}{t}|x\rangle,\ \text{and}\ |y'\rangle = \frac{1}{\sqrt{1-t^2}}|y\rangle.$$

Then $\langle x'|x'\rangle = \langle y'|y'\rangle = 1$ and

$$\langle v|M|v\rangle = t\langle x'|M|x'\rangle + (1-t)\langle y'|M|y'\rangle\,. \tag{38}$$

That is, the extreme points of $\Lambda(M_1, M_2, M_3)$ lie in $\Lambda_{\mathbb{R}}(M_1, M_2, M_3) = \Pi_+(H_1, H_2, H_3)$. Since $\Lambda(M_1, M_2, M_3)$ is convex and the convex hull of $\Pi_+(H_1, H_2, H_3)$ is $\Theta_+(H_1, H_2, H_3)$, we have

Observation 3

$$\Theta_+(H_1, H_2, H_3) = \Lambda(M_1, M_2, M_3)\,. \tag{39}$$

$\Lambda(M_1, M_2, M_3)$ has been classified in [34]. Ours is a subcase where M_1, M_2, M_3 are all real. From Fig. 1 of [34], the only possible shapes of the ruled surfaces on $\partial\Theta_+(H_1, H_2, H_3)$ is a cone shape.

A cone-shape $\Theta_+(H_1, H_2, H_3)$ can be given by block diagonal M_is, for example $d_{xz,i} = d_{yz,i} = 0$. For a concrete example, take

$$M_1 = \begin{pmatrix} 1 & 0 & 0 \\ 0 & -1 & 0 \\ 0 & 0 & 0 \end{pmatrix}, M_2 = \begin{pmatrix} 0 & 1 & 0 \\ 1 & 0 & 0 \\ 0 & 0 & 0 \end{pmatrix}, M_3 = \begin{pmatrix} 0 & 0 & 0 \\ 0 & 0 & 0 \\ 0 & 0 & 1 \end{pmatrix}.$$

The corresponding Hamiltonian is given by

$$\begin{aligned} H_1 &= X\otimes X - Y\otimes Y, \\ H_2 &= X\otimes Y + Y\otimes X, \\ H_3 &= Z\otimes Z\,. \end{aligned} \tag{40}$$

The joint product numerical range $\Pi_+(H_1, H_2, H_3)$ has the form as shown in Fig. 5.

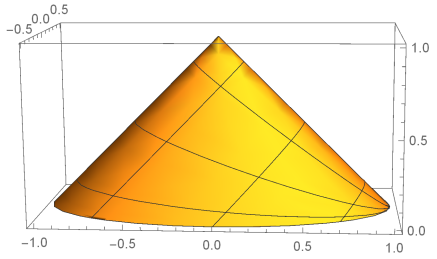

FIG. 5. A cone shape $\Pi_+(H_1, H_2, H_3)$.

B. The non-homogenous case

For the non-homogenous case (i.e. f_is are not homogenous polynomials of r, s, t), we look at the two examples discussed in [14], which are many-body interacting boson systems in the $N \to \infty$ limit. The first example is the two model Ising model with

$$H_1 = X \otimes X\,,$$
$$H_2 = \frac{1}{2}(Z \otimes I + I \otimes Z)\,,$$
$$H_3 = \frac{1}{2}(X \otimes I + I \otimes X)\,. \tag{41}$$

This corresponds to

$$f_1 = r^2,\ f_2 = t,\ f_3 = r, \tag{42}$$

as formulated in Eq. (28).

The joint product numerical range $\Pi_+(H_1, H_2, H_3)$ has the form as in Fig. 6. This corresponds to the blue ruled

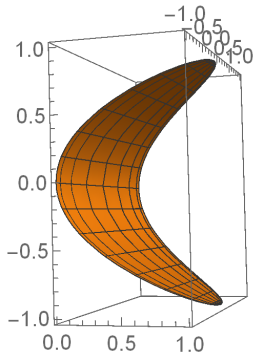

FIG. 6. $\Pi_+(H_1, H_2, H_3)$ for the two mode Ising model.

surface of Fig. 1 in [14], which has a gapless physical origin. The green ruled surface of Fig. 1 in [14] is a result of the convex hull of $\Pi_+(H_1, H_2, H_3)$, which corresponds to symmetry-breaking.

The second example in [14] is the two model XY model with

$$H_1 = X \otimes X\,,$$
$$H_2 = Y \otimes Y\,,$$
$$H_3 = \frac{1}{2}(Z \otimes I + I \otimes Z)\,. \tag{43}$$

This corresponds to

$$f_1 = r^2,\ f_2 = s^2,\ f_3 = t, \tag{44}$$

as formulated in Eq. (28).

The joint product numerical range $\Pi_+(H_1, H_2, H_3)$ has the form as shown in Fig. 7. This corresponds to the blue ruled surface of Fig. 4 in [14], which has a gapless physical origin.

These examples support our idea that a ruled surface on $\partial\Theta_+(H_1, H_2, H_3) \cap \Pi_+(H_1, H_2, H_3)$ have a gapless origin, as discussed in Sec. IIIA.

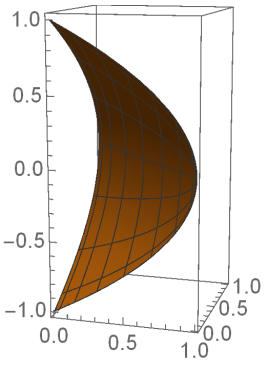

FIG. 7. $\Pi_+(H_1, H_2, H_3)$ for the two mode XY model.

V. SUMMARY AND DISCUSSION

In this work, we make a connection between joint product numerical range and reduced density matrix geometry. We focus on the case of systems in infinite spatial dimension, where the reduced density matrices are known to be separable due to the quantum de Finetti's theorem. In this scenario, our main observation is that the intersection of the joint product numerical range $\Pi(H_1, H_2, H_3)/\Pi_+(H_1, H_2, H_3)$ with the boundary of its convex hull $\Theta(H_1, H_2, H_3)/\Theta_+(H_1, H_2, H_3)$ contains information on the physical properties of the system. In particularly, a ruled surface on $\partial\Theta(H_1, H_2, H_3)$ that is in $\Pi(H_1, H_2, H_3)$ has a gapless origin, otherwise it has a symmetry breaking origin.

Notice that it is possible to have the same $\Theta(H_1, H_2, H_3)/\Theta_+(H_1, H_2, H_3)$ that is the convex hull obtained from very different $\Pi(H_1, H_2, H_3)\Pi_+(H_1, H_2, H_3)$. We provide some concrete examples in Appendix A. Similar ideas apply to the case of the same $\Theta_+(H_1, H_2, H_3)$ with different $\Pi_+(H_1, H_2, H_3)$. Therefore, in practice, solely by looking at the shape of $\Theta(H_1, H_2, H_3)$ is not enough to tell the physical properties of the system. One will need to further look at the shape of $\Pi(H_1, H_2, H_3)$, especially its intersection with $\partial\Theta(H_1, H_2, H_3)$.

We provide a general method to obtain ruled surfaces on $\Theta(H_1, H_2, H_3)$, where $\Theta(H_1, H_2, H_3)$ is a convex hull of two convex objects. This allows us to construct $\Theta(H_1, H_2, H_3)$ of certain interesting geometric shapes, such as the oloid. Similar idea is applied to the symmetric case where different shapes of ruled surfaces $\Theta(H_1, H_2, H_3)$ are obtained.

It will be interesting to classify all possible shapes of the joint separable numerical range $\Theta(H_1, H_2, H_3)/\Theta_+(H_1, H_2, H_3)$, and the corresponding joint separable numerical range $\Pi(H_1, H_2, H_3)/\Pi_+(H_1, H_2, H_3)$, at least in low (single-particle) dimensions, for systems with infinite spatial dimension where the quantum de Finetti's theorem is

valid. That will then contain information of all possible physical properties in these systems.

ACKNOWLEDGEMENT

NY and BZ are supported by NSERC and CIFAR. This research was supported in part by Perimeter Institute for Theoretical Physics. Research at Perimeter Institute is supported by the Government of Canada through Industry Canada and by the Province of Ontario through the Ministry of Economic Development & Innovation.

Appendix A. $\Theta(H_1, H_2, H_3)$ vs. $\Pi(H_1, H_2, H_3)$

Let

$$X = \begin{pmatrix} 0 & 1 \\ 1 & 0 \end{pmatrix}, \; Y = \begin{pmatrix} 0 & -i \\ i & 0 \end{pmatrix}, \; Z = \begin{pmatrix} 1 & 0 \\ 0 & -1 \end{pmatrix}.$$

The following three examples all have the same $\Theta_+(H_1, H_2, H_3)$.

Example 1 Let $H_1 = (I + Z) \oplus (-I + Z)$, $H_2 = X \oplus X$ and $H_3 = Y \oplus Y$. Then

$$\begin{aligned} &\Pi(H_1, H_2, H_3) = \\ &\{(2t - 1 + \cos\theta, \sin\theta\cos\phi, \sin\theta\sin\phi) : \\ &0 \le t \le 1, \; 0 \le \theta, \; \phi \le 2\pi\} \\ &= \Theta(H_1, H_2, H_3)\,. \end{aligned}$$

The corresponding $\Pi(H_1, H_2, H_3)$ is shown in Fig. 8. Since the boundary ruled surface of $\Theta(H_1, H_2, H_3)$ is

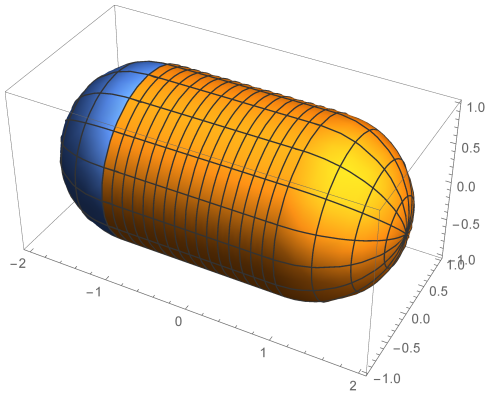

FIG. 8. $\Pi(H_1, H_2, H_3)$ for Example 1.

in $\Pi(H_1, H_2, H_3)$, it has a gapless origin as discussed in Sec. IIIA.

Example 2 Let $H_1 = (I+Z)\oplus(-I+Z)$, $H_2 = X\oplus(-X)$ and $H_3 = Y \oplus (-Y)$. Then

$$\begin{aligned} &\Pi(H_1, H_2, H_3) = \\ &\{(2t - 1 + \cos\theta, (2t-1)\sin\theta\cos\phi, (2t-1)\sin\theta\sin\phi) : \\ &0 \le t \le 1, \; 0 \le \theta, \; \phi \le 2\pi\}\,. \end{aligned}$$

The corresponding $\Pi(H_1, H_2, H_3)$ is shown in Fig. 9. Since the boundary ruled surface of $\Theta(H_1, H_2, H_3)$ is not

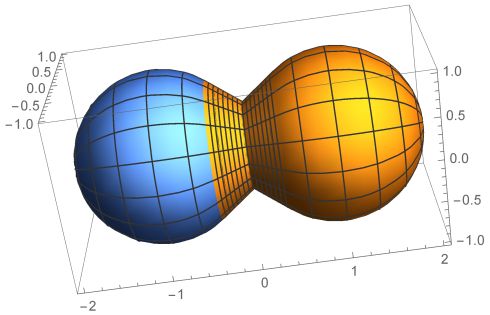

FIG. 9. $\Pi(H_1, H_2, H_3)$ for Example 2.

in $\Pi(H_1, H_2, H_3)$, it has a symmetry breaking origin as discussed in Sec. IIIA.

Example 3 Let $H_1 = (I+Z)\oplus(-I-Z)$, $H_2 = X\oplus(-X)$ and $H_3 = Y \oplus (-Y)$. Then

$$\begin{aligned} &\Pi(H_1, H_2, H_3) = \\ &\{((2t - 1)\cos\theta, (2t-1)\sin\theta\cos\phi, (2t-1)\sin\theta\sin\phi) : \\ &0 \le t \le 1, \; 0 \le \theta, \; \phi \le 2\pi\}\,. \end{aligned}$$

The corresponding $\Pi(H_1, H_2, H_3)$ is shown in Fig. 10. Since the boundary ruled surface of $\Theta(H_1, H_2, H_3)$ is not

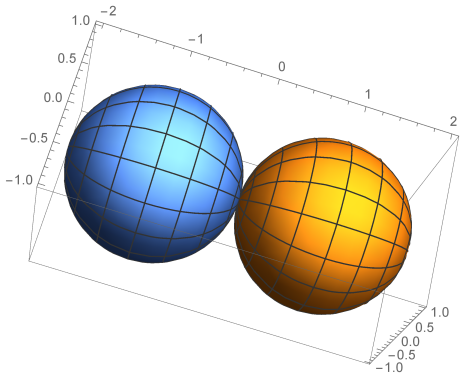

FIG. 10. $\Pi(H_1, H_2, H_3)$ for Example 3.

in $\Pi(H_1, H_2, H_3)$, similar to Example 2, it has a symmetry breaking origin.

[1] A. J. Coleman, Rev. Mod. Phys. **35**, 668 (1963).
[2] R. M. Erdahl, Journal of Mathematical Physics **13**, 1608 (1972).
[3] A. A. Klyachko, in *Journal of Physics: Conference Series*, Vol. 36 (IOP Publishing, 2006) p. 72.
[4] R. Erdahl and B. Jin, in *Many-Electron Densities and Reduced Density Matrices*, Mathematical and Computational Chemistry, edited by J. Cioslowski (Springer US, 2000) pp. 57–84.

[5] C. A. Schwerdtfeger and D. A. Mazziotti, The Journal of Chemical Physics **130**, 224102 (2009).

[6] Y.-K. Liu, in *Approximation, Randomization, and Combinatorial Optimization. Algorithms and Techniques*, Lecture Notes in Computer Science, Vol. 4110, edited by J. Diaz, K. Jansen, J. D. Rolim, and U. Zwick (Springer Berlin Heidelberg, 2006) pp. 438–449.

[7] Y.-K. Liu, M. Christandl, and F. Verstraete, Phys. Rev. Lett. **98**, 110503 (2007).

[8] T.-C. Wei, M. Mosca, and A. Nayak, Phys. Rev. Lett. **104**, 040501 (2010).

[9] F. Verstraete and J. I. Cirac, Phys. Rev. B **73**, 094423 (2006).

[10] G. Gidofalvi and D. A. Mazziotti, Phys. Rev. A **74**, 012501 (2006).

[11] J. Chen, Z. Ji, C.-K. Li, Y.-T. Poon, Y. Shen, N. Yu, B. Zeng, and D. Zhou, New Journal of Physics **17**, 083019 (2015).

[12] V. Zauner, L. Vanderstraeten, D. Draxler, Y. Lee, and F. Verstraete, arXiv preprint arXiv:1412.7642 (2014).

[13] J.-Y. Chen, Z. Ji, Z.-X. Liu, Y. Shen, and B. Zeng, Physical Review A **93**, 012309 (2016).

[14] J.-Y. Chen, Z. Ji, Z.-X. Liu, X. Qi, N. Yu, B. Zeng, and D. Zhou, arXiv preprint arXiv:1605.06357 (2016).

[15] J. W. Gibbs, Transcations of the Connecticut Academy **2**, 309 (1873).

[16] J. W. Gibbs, Transcations of the Connecticut Academy **2**, 382 (1873).

[17] J. W. Gibbs, Transcations of the Connecticut Academy **3**, 108 (1875).

[18] R. B. Israel, *Convexity in the Theory of Lattice Gases* (Princeton University Press, 1979).

[19] E. Stormer, Journal of Functional Analysis **3**, 48 (1969).

[20] R. L. Hudson and G. R. Moody, Probability Theory and Related Fields **33**, 343 (1976).

[21] M. Lewin, P. T. Nam, and N. Rougerie, Advances in Mathematics **254**, 570 (2014).

[22] Z. Puchala, P. Gawron, J. A. Miszczak, L. Skowronek, M.-D. Choi, and K. Życzkowski, Linear Algebra and its Applications **434**, 327 (2011).

[23] G. Dirr, U. Helmke, M. Kleinsteuber, and T. Schulte-Herbrüggen, Linear and Multilinear Algebra **56**, 27 (2008).

[24] R. Duan, Y. Feng, and M. Ying, Physical review letters **100**, 020503 (2008).

[25] T. Schulte-Herbruggen, G. Dirr, U. Helmke, and S. J. Glaser, Linear and Multilinear Algebra **56**, 3 (2008).

[26] T. Schulte-Herbruggen, S. J. Glaser, G. Dirr, and U. Helmke, Reviews in Mathematical Physics **22**, 597 (2010).

[27] P. Gawron, Z. Puchala, J. A. Miszczak, L. Skowronek, and K. Zyczkowski, Journal of Mathematical Physics **51**, 102204 (2010).

[28] B. Zeng, X. Chen, D.-L. Zhou, and X.-G. Wen, arXiv preprint arXiv:1508.02595 (2015).

[29] Y.-H. Au-Yeung and Y.-T. Poon, SEA Bull. Math. **3**, 85 (1979).

[30] P. Gawrona, Z. Puchala, J. A. Miszczak, S. Lukasz, and M.-D. Choi, Linear Algebra and its Applications **434**, 327 (2011).

[31] J. Chen, Z. Ji, B. Zeng, and D. Zhou, Physical Review A **86**, 022339 (2012).

[32] P. Binding and C.-K. Li, Linear Algebra and its Applications **151**, 157 (1991).

[33] H. Dirnböck and H. Stachel, Journal for Geometry and Graphics **1**, 105 (1997).

[34] K. Szymański, S. Weis, and K. Życzkowski, arXiv preprint arXiv:1603.06569 (2016).